Int. J. Rock Mech. Min. Sci. & Geomech. Abstr. Vol. 12, pp. 283–288. Pergamon Press 1975. Printed in Great Britain

Shaped Charge Sequencing*†

M. VAN THIEL‡
M. WILKINS
A. MITCHELL

A method is proposed for using sequentially-fired, shaped charges to drill deep, small-diameter holes in rock more efficiently. Using this method, penetration in igneous rock can be increased from 10 times the diameter of a single, copper-lined charge to 18 or more times this diameter when two or more charges are fired sequentially. Design calculations for a shaped-charge drilling system can be performed using Bernoulli's equation; however, this simple mathematical model has several shortcomings. Shaped-charge penetration, therefore, should be computed using a scaling technique and available experimental data. This allows the penetration efficiency of a sequence of shaped charges to be determined. A shaped-charge drilling device is presented which uses two or more staged charges. Hydrodynamic evaluation of this device, especially the mechanics of slug deflection, indicates that this design overcomes some of the weaknesses of earlier designs. A major improvement is the use of explosive cylindrical lenses, initiated by mild detonating delay fuses, to ensure proper symmetrical firing of the second- and third-stage explosives.

INTRODUCTION

Shaped-charge drilling, the most rapid drilling process known, is a spinoff from World War II technology development. A shaped charge is an explosive with a metal-lined, hemispherical-, wedge-, or conical-shaped cavity. Detonation collapses this cavity, ejecting a supersonic stream of metal called the jet [1]. Drilling speeds of 2–6 km/sec and hole depths of 4–15 times charge diameter can be achieved using shaped charges. Despite this tremendous potential for mining applications, shaped charges are used primarily in cutting and perforating metal. Their potential for tunneling and blasting work should be considered seriously, since such explosives provide a very concentrated energy source. The shaped charge lends itself to remote mining operations where noise is not an important factor.

High-velocity penetration of solid materials, as opposed to slow mechanical drilling or ballistic penetration, involves the melting and vaporization of the target. As a result, penetration depth is little dependent on the strength of the material being penetrated. Simple scaling laws, therefore, can be used quite effectively in predicting relative jet effectiveness in penetrating different materials.

THEORY

Simple model

The most conceptually useful description of target penetration by a shaped-charge jet (Fig. 1) and, for most purposes, a reasonably good one is based on Bernoulli's equation

$$\frac{\partial p}{\rho} + \tfrac{1}{2}U^2 = \text{constant} \simeq \frac{p}{\bar{\rho}} + \tfrac{1}{2}U^2, \tag{1}$$

where p is pressure, ρ is density, and U is velocity. The last term of this equation is based on the assumption that the target material compresses only slightly or not at all during the process. Then, following Birkhoff *et al.* [1] the equation can be rewritten as

$$\tfrac{1}{2}\rho_j(V - U)^2 = \tfrac{1}{2}\rho U^2, \tag{2}$$

where ρ is the density and U the velocity of the target material at the jet-target interface and V is initial velocity of the jet with a density ρ_j (see Fig. 1). Since penetration time (Δt) is the time it takes for the rear end of the jet to reach the moving interface,

$$\Delta t = \frac{l}{V - U} \tag{3}$$

and, using equation (3), we represent penetration by

$$P = U\Delta t = l\frac{U}{V - U} = l \cdot \left(\frac{\rho_j}{\rho}\right)^{1/2}. \tag{4}$$

* Work performed under the auspices of the U.S. Energy Research and Development Administration and supported in part by the Advanced Research Projects Agency.

† This report was prepared as an account of work sponsored by the United States Government. Neither the United States nor the United States Energy Research and Development Administration, nor any of their employees, nor any of their contractors, subcontractors, or their employees, makes any warranty, express or implied, or assumes any legal liability or responsibility for the accuracy, completeness or usefulness of any information, apparatus, product or process disclosed, or represents that its use would not infringe privately owned rights.

‡ Lawrence Livermore Laboratory, University of California, Livermore, CA 94550, U.S.A.

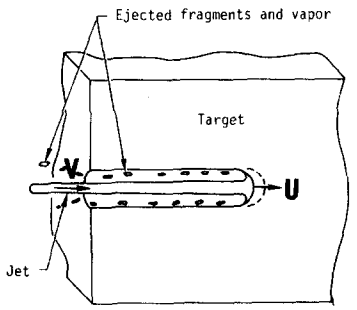

Fig. 1. Diagram of idealized jet penetration (V = jet velocity; U = penetration rate).

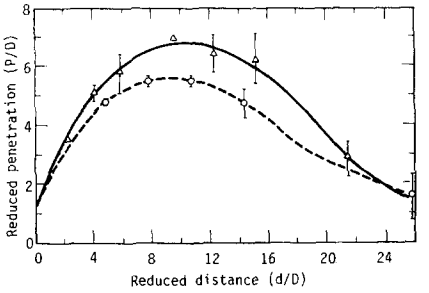

Fig. 2. Shaped charge performance (copper cones and steel target): penetration vs charge to center of hole in cone-base diameters (· = Octol explosive; Δ = HMX-based extrudable explosive).

Penetration depth, therefore, depends only on jet length.

Approximations

The penetration model just described is not completely accurate for several reasons. One, the jets produced from shaped charges do not have a constant velocity along their length [2]. This means jet length changes with time or travel distance, so that the jet eventually breaks up into a number of elongated particles, each acting as an individual penetrator. These particles, in turn, begin to tumble, thereby reducing their penetration capacity. Breakup and tumbling are the results of perturbing oscillations produced in jet formation and turbulent interactions with surrounding gasses, respectively. These factors are not taken into account in the simple penetraton model.

The shape of the jet particles also affect jet length and, hence, penetration depth. Particle shape depends on the material used for the liner. X-ray shadowgraphs [3] indicate that an iron liner breaks up like a brittle material, forming jagged particles; while copper appears more ductile, breaking up into elongated particles. Aluminum jets, on the other hand, appear like a spray of particles down to submillimeter size probably with smaller, unresolved particles in between. This suggests partial melting of the aluminum.

Finally, the model ignores the transfer of momentum from material ejected from the target hole to the impinging jet. It also ignores viscosity effects at the target–jet interface.

Jet length

The fact that jet velocity is not constant and jet length varies with time and distance increases the value of l in equation (4) with time. The resulting increase in penetration capacity with increased standoff (distance between charge and target) is well known [1]. Penetration–vs–standoff curves have the following general shape: an initial increase of penetration (P) as charge and target are separated, with maximum penetration occurring at separations between 7–10 cone-base diameters, followed by a decrease in penetration with greater standoff distances.

The performance of a precision-machined copper cone has been examined experimentally using several different explosives. As shown in Fig. 2, Octol and a (60:40≡) RDX: TNT mixture both yield jets with about the same steel penetration capacities [4]. Important to note is the decrease in efficiency as charge-to-target distance is increased. A similar effect was found using a more energetic charge of extrudable HMX-base explosive developed at Lawrence Livermore Laboratory [5]. However, in this latter case, performance improved at nominal standoff distances and dropped off slightly faster at greater distances. The flags in Fig. 2 indicate the range of penetrations obtained from three or more charges. This variability shows the importance of quality control. Ideally, it should be possible to predict penetration into any other target by scaling these data with equation (4) but minor deviations may be expected in low-density targets.

Parameterization

A variety of parametric equations to account for jet lengthening and breakup [1,2], change of cross sectional areas [1], and target strength [6,7] have been formulated and compared with experimental data. Detailed X-ray analysis of jet penetration [8,9] has shown that jet length increases to the time of breakup and that subsequent particle length (hence, effective jet length) remains constant. The latter holds true up to the time that the jet particles start to tumble, reducing the effective value of l. A strength factor was introduced by an empirical determination of the jet particle velocity below which no penetration occurs. It must be noted that this limiting velocity is not only a function of target strength, but also of target density and standoff (as may be inferred from the above discussion and equation (4)). Penetration data indicate, however, that target strength is not an important variable in describing variations between materials.

Alternate approach

A detailed analysis of the penetration [10] process has been made with limited success [9]. Actual penetration is considerably smaller than that predicted by this simple theory, which accounts for jet length variations and breakup, but not the other limitations of equation (4). A somewhat different approach to comparing penetration through materials with different

densities is to rewrite equation (4) in the form

$$\delta P = (\rho_j/\rho_{st})^{\frac{1}{2}}\, \delta l^{\text{eff}}(d), \tag{5}$$

recognizing the fact that efficiency is a function of distance and that we wish to use a value of $l(=l^{\text{eff}})$ consistent with observed penetration yet smaller than the actual value of l. It is convenient to make comparisons to the peak of the P/D-vs-d/D curve in Fig. 2; a numerical method is employed to avoid fitting bell-shaped curves.

Considering the penetration of n sections of jet, each of length $\delta l^{\text{eff}}(d)$, we get

$$p_{st} \sum \delta P_{st}(d_i) = \sum (\rho_j/\rho_{st})^{1/2} \,.\, \delta l^{\text{eff}}(d_i). \tag{6}$$

Now, realizing that the value of δl^{eff} is a maximum at some value of $d = d_1$, we may for any real process calculate a maximum penetration ($P^{\max}$) by normalizing each term by

$$\alpha(d) = \frac{\delta l^{\text{eff}}(d_1)}{\delta l^{\text{eff}}(d)} = \frac{P_{st}(d_1)}{P_{st}(d)},$$

which can be calculated from the steel penetration curve (Fig. 2) with reasonable accuracy. Therefore,

$$P_{st}^{\max} = \sum_{i=1}^{n} (\rho_j/\rho_{st})^{1/2} \,.\, \delta l^{\text{eff}}(d_i) \,.\, \alpha(d_i) \tag{7}$$

represents this maximum penetration in steel, which may be compared to the penetration through any material (m) by multiplying the terms by $(\rho_m/\rho_m)^{1/2}$. We can now write the penetration-scaling equation between steel and material m as

$$P_{st}^{\max} = \sum_{i=1}^{n} (\rho_j/\rho_m)^{1/2} \,.\, (\rho_m/\rho_{st})^{1/2} \,.\, \delta l^{\text{eff}}(d_i) \,.\, \alpha(d_i)$$

$$= \sum_{i=1}^{n} \beta_m \,.\, \delta P_m(d_i) \,.\, \alpha(d_i), \tag{8}$$

where, in the last sum, $\beta_m = (\rho_m/\rho_{st})^{1/2}$ and δP_m is the incremental penetration of the material in question.

EXPERIMENTAL CHECK

To test equation (8) in an extreme case, a precision charge like that shown in Fig. 2 was fired through a 0·61-m column of water into a stack of steel plates. The cone-base diameter was 0·053 m. Penetration and jet configuration were monitored by X-ray shadowgraphs. In addition, penetration was monitored with a set of charged foil switches that recorded the position of the jet tip at various times. The experimental setup, including significant dimensions, is shown schematically in Fig. 3. A simple device called the virtual origin approximation [9] allows us to calculate the position of the jet particles quickly as a function of time. This surprisingly accurate calculation assumes that all particles start at the same time from a common origin. The progress of the jet particles through the water and steel layers is shown by the dashed lines in Fig. 4. The

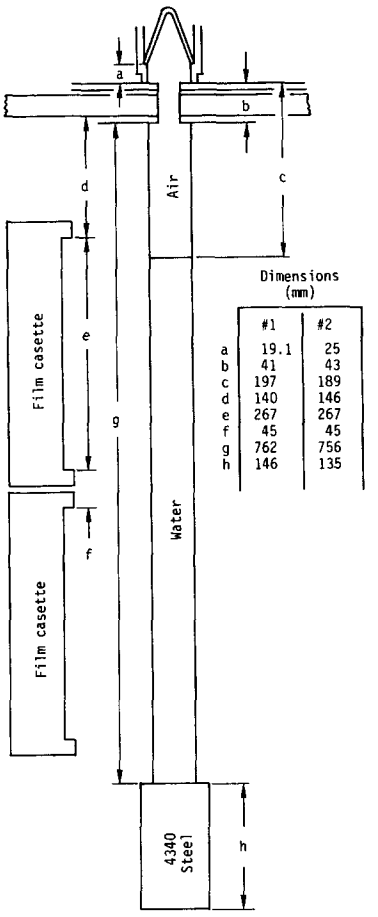

Fig. 3. Schematic of penetration tests.

position of the jet tip, obtained directly from foil switch closing times, also is shown. This position can be inferred, in part, from the X-ray shadowgraphs that are superimposed on the graph. These shadowgraphs correlate well with the penetration locus given by the foil switches and show the shape of the particles.

Now, equation (8) can be used to calculate maximum penetration into the steel from the above experiment for comparison with Fig. 2. Using $\beta_w = 0{\cdot}357$ and taking α from Fig. 2, we get $p_{st}^{\max} = 7.00$, in good agreement with Fig. 2. A word of caution must be added, however. In extrapolating penetration in steel to that in water or rocks, allowance must be made for the difference in the fraction of the jet effective in penetration. In the above example, this cutoff was at a jet velocity of 4 km/sec (see Fig. 4). But this holds for the penetration through steel. For soft, low-melting point materials the cutoff velocity will be lower and effective penetration higher, an important factor especially in soft or hydrated and water-bearing rocks.

To estimate the effective penetration depth of a sequence of charges in material other than steel (e.g. rock of density 3 g/cm^3), we modified equation (8) and the graph in Fig. 2 by rewriting the left side of the equation as

$$\sum_{i=1}^{n} \delta P_{st}^{\max} \text{ such that } \delta P_{st}^{\max} = \frac{P_{st}^{\max}}{n}. \tag{9}$$

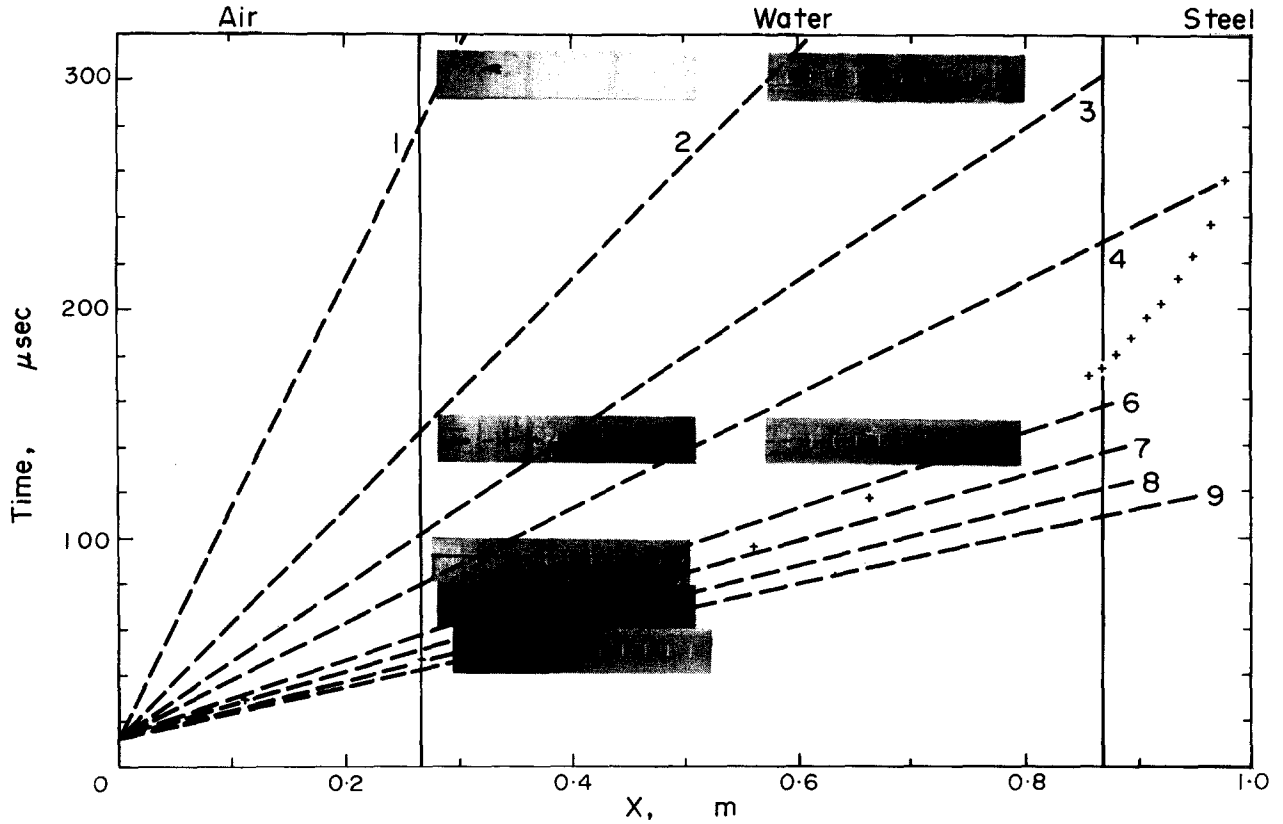

Fig. 4. Jet characteristics in water and steel; dashed line shows position of jet particles vs time in the virtual origin approximation; plus signs indicate foil switch signals produced by jet tip passage; dots represent jet particles.

Equating terms, dividing through by α and β, and summing we get

$$P_m = \sum_{i=1}^{n} \delta P_m = (n \cdot \beta_m)^{-1} \cdot \sum_{i=1}^{n} \frac{\delta P_{st}^{\max}}{\alpha(d_i)}, \qquad (10)$$

where

$$d_p = X_o + \frac{1}{\beta_m}\left[\left\{\sum_{i=1}^{p-1} \frac{P_{st}^{\max}}{n \cdot \alpha(d_i)}\right\} + \frac{P_{st}^{\max}}{2n \cdot \alpha(d_p)}\right].$$

A reasonably good estimate may be made with $n = 1$ or 2. The first of a sequence of 50 mm-dia charges would penetrate 0·5 m, the second stage an additional 0·4 m, and a third charge an additional 0·2 m; making total penetration for the two-stage device 0·9 m or 18 diameters and for the three-stage device 1·1 m or 22 diameters. The limitation of multistage drilling devices clearly is the reduction of penetration as a function of distance.

STAGING CONCEPT

Hole size and drilling depth can be controlled to some extent by standoff and cone size. Increased standoff decreases hole diameter but increases hole depth (up to a maximum distance of 10 cone diameters). Increasing cone size increases both diameter and depth of the hole. For many applications, however, increased penetration is more important than increased diameter. Furthermore, where space or total explosive weight are limitations, staged charges (i.e. firing in sequence a row of carefully aligned charges) should be considered [4].

A number of staged, shaped-charge drilling techniques have been proposed. See, for example, U.S. patent: 3,215,074 (2 Nov. 1965); 3,375,108 (26 March 1968); and 3,416,449 (17 Dec. 1968). The multistage drilling device shown in Fig. 4 uses a normal conical-shaped charge (A) with a 42° apex angle and as many charges with hollow truncated cones (B) as the application and ultimate design require. The firing sequence is as follows: charge A is detonated by a single detonator centered on the exposed end of the explosive charge (not shown). This detonation collapses the metal cone, which forms a jet that passes through the central tube of the slug catcher between charges A and B. The detonation wave from charge A ignites an explosive delay train, which lights an explosive charge in the slug catcher, trapping the slow part of the jet after the main portion of the jet has passed. Meanwhile, the explosive fuse train burns on to light another explosive delay coil that, in turn, ignites a cylindrical lens which initiates a symmetrical detonation wave in the second shaped charge B. The process, in principle, may be repeated for additional charges.

The device can be sealed and evacuated to eliminate the perturbing effects of air shocks; however, there are some problems yet to be solved. These include:

1. Removal of the slow part of the jet (slug catching);
2. Mechanical isolation of charges to prevent unwanted shock deformations and preinitiation of neighboring charges;
3. Proper initiation of the sequenced charges.

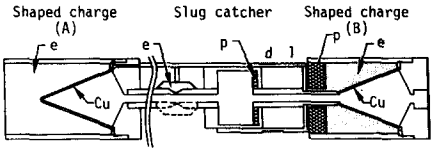

Fig. 5. Schematic of multistage, shaped-charge drilling device (e = explosive; Cu = copper cone; p = porous metal shock attenuator; d = mild-detonation-fuse delay coil; l = cylindrical explosive lens).

SLUG CATCHER PROBLEM

The slug catcher design shown in Fig. 5 is schematic only. Neither the central tube, the explosive, nor the shape of other downstream parts need to be cylindrically symmetric. Furthermore, few materials of practical interest exist that can be penetrated by copper jet particles moving at 2 km/sec. In fact, at this low velocity the trailing metal (slug) tends to fill the hole made by the fast portion of the jet. The slug catcher, therefore, must be designed to trap a high-density metal stream flowing at up to 4 km/sec, recognizing the fact that much of the metal cone ($\simeq$60–70%) is accelerated to velocities between 1 and 4 km/sec.

If the slow portion of the jet is to be trapped by symmetrically compressing the tube, the energy density and momentum of that part of the jet must be considered very carefully. Copper jet speeds of 3·5 km/sec or greater are required to penetrate steel. Slug trapping by symmetric tube closure around a jet depends on the viscous transfer of momentum to the tube from the jet stream either close to its melting point or in the liquid phase. This viscous deceleration process requires a relatively large amount of explosive to maintain tube pressure during the deceleration period. One way to increase the deceleration rate is to shape the charge to give material surrounding the jet a velocity component in the opposite direction of the jet. This method, however, requires a comparatively large amount of explosive. In addition, the design complexities involved could double system costs.

A better approach is to introduce a small amount of momentum perpendicular to the jet to deflect it against a sufficiently heavy mass. A simple way to cause such deflection is to detonate asymmetrically a cylinder of explosive around the steel tube through which the jet passes towards the second stage (see Fig. 5). This design technique was tested by calculation and experiment. The calculations were performed using a lagrange hydrodynamic code [11], which followed the behavior of all significant parts of the system as the explosive detonated, compressed, and accelerated surrounding parts. This calculated behavior at the start of detonation and when the hole is almost closed is shown in Fig. 6. The deflection of the tube from its axis is small for the design dimensions chosen. This small deflection was also confirmed by experiment. In fact, recovered samples suggest that later in time tube deflection decreases slightly.

A more effective design is depicted in cross-section in Fig. 7. This is a calculation of the movement of

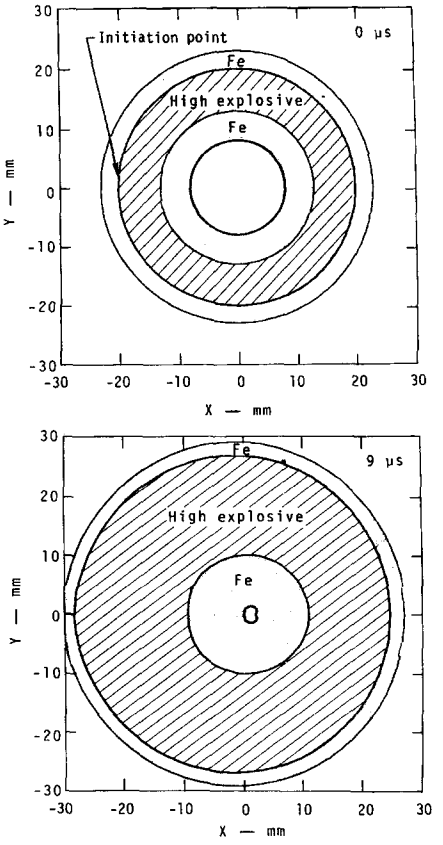

Fig. 6. Calculated implosion of a solid iron pipe using asymmetric explosive initiation.

a slotted cylindrical system of explosive and steel. The particular configuration chosen for the calculation results in the central jet being enveloped by the tube. The choice of slot angle or shape is clearly in question here and depends to some extent on the overall design. In any case, the central jet material reached a radial velocity of 1 km/sec, 5·5 μsec after detonating the catcher explosive. This is more than enough velocity

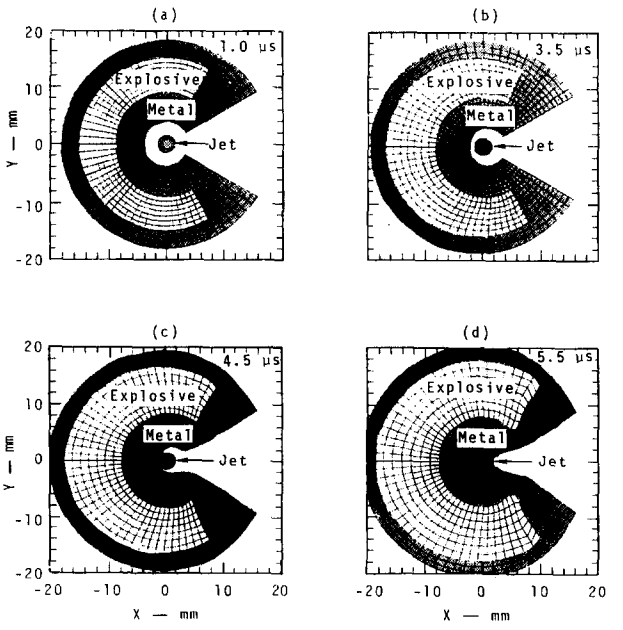

Fig. 7. Calculated jet deflection by a slotted catcher system.

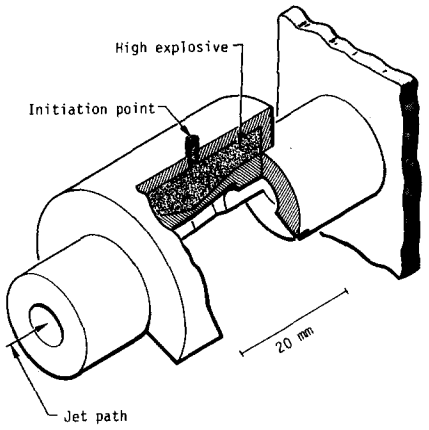

Fig. 8. Slotted slug catcher configuration.

for jet deflection. This shape, therefore, appears to be a good guide for the design.

An important consideration is the effect that severing the rear part of the jet could have on the remaining portion. Some of the jet material will be partially deflected. The design challenge is to minimize this effect.

A second consideration is the strength of the catcher material after deformation by the explosive. This is important because it must withstand the impact of massive, slow-moving slug fragments that could reopen the jet flight path and exposing the second stage to slow debris. Final slug catcher design must account for both of these possibilities. A reasonably simple, but adequate, design of a slotted catcher system is shown in Fig. 8.

SECOND-STAGE INITIATION

If protected from debris, the second stage can be detonated symmetrically and in proper alignment with the first stage. This second-stage initiation can be accomplished in two ways. If limited space is not an important factor and a high-voltage source is readily available, the second stage can be initiated using a ring of detonators. This method, however, is bulky and cumbersome to use under field conditions. The second method is to use mild detonating fuse between the two stages and an explosive lens to ignite the second stage symmetrically at 10 or more points on a ring around the charge. In addition to being more compact, the cost of handling and deploying this system should be lower. Moreover, since the lens consists of a system of grooves cast in a plastic cylinder and filled with extrudable or plastic explosive, it readily lends itself to the economies of mass production.

SUMMARY

This study shows that the drilling performance of shaped charges can be improved significantly by staging the charges and firing them in sequence. Based on hydrodynamic calculations and actual experimental tests, a multistage, shaped-charge drilling device is proposed that satisfies the design restrictions imposed by metal jet behavior. These design calculations also demonstrate the value of hydrodynamic computer codes in designing drilling systems of this type. Finally, an analytical method is developed and evaluated, which allows shaped-charge drilling performance to be scaled to a wide range of target materials.

Acknowledgements—The authors wish to extend their appreciation to Nora Wilt and Dick Giroux for their help in these calculations, to John Hallam for providing the shaped charges for the tests, and to Chuck Henry and Earl Thompson for their useful inputs on explosive lens design.

Received 10 *February* 1975.

REFERENCES

1. Birkhoff G., McDougall D. P., Pugh E. M. and Taylor Sir G. Explosives with lined cavities. *J. appl. Phys.* **19**, 563 (1948).
2. Pugh E. M., Eichelberger R. J. and Rostocker N. J. Theory of jet formation by charges with lined conical cavities. *J. appl. Phys.* **23**, 532 (1952).
3. Kennedy D. R. Private communication. Food Machinery Co., San Jose, CA (1974).
4. Breidenbach H. I. Ballistic Research Laboratory, Report 848 (declassified), Defense Document Center, Cameron Station, Alexandria, VA (1953).
5. Walker F. E. Participation of LLL in TSEXP, Part B: Characterization of ECX for conventional munitions. Lawrence Livermore Laboratory, Report UCID-16557, p. 75ff, Livermore, CA (1974). [Also, Hallam J. Private communication. Lawrence Livermore Laboratory, Livermore, CA (1974).]
6. Pack D. C. and Evans W. M. Penetration by high velocity (Munroe) jets: part I. *Phys. Soc. (London) Proc.* **B64**, 298 (1951).
7. Eichelberger R. J. Experimental test of the theory of penetration by metallic jets. *J. appl. Phys.* **27**, 63 (1956).
8. Simon J. and Dipersio R. Experimental verification of standoff effects on shaped charge jet cutoff in solid targets. Ballistic Research Laboratory, Report. MR1976, Aberdeen Proving Ground, MD (1969).
9. Dipersio R., Simon J. and Merindo A. B. Penetration of shaped-charge jets into metallic targets. Ballistic Research Laboratory, Report R1296, Aberdeen Proving Ground, MD (1965).
10. Allison F. E. and Vitchi R. A new method of computing penetration variables for shaped-charge jets. Ballistic Research Laboratory, Report BRL1184, Aberdeen Proving Ground, MD (1963).
11. Wilkins M. L. Calculation of elastic–plastic flow. Lawrence Livermore Laboratory, Report UCRL-7322, Livermore, CA (1969).